JOURNAL OF MATERIALS SCIENCE **34** (1999) 4639–4644

Formation region of monophase with cubic spinel-type oxides in Mn–Co–Ni ternary system

Y. ABE
Technol Seven Co., Ltd., 1-3-13 Kamoi, Midori-ku, Yokohama-shi 226-0003, Japan
T. MEGURO, S. OYAMATSU, T. YOKOYAMA, K. KOMEYA
Yokohama National University, 79-5 Tokiwadai, Hodogaya-ku, Yokohama-shi 240-8501, Japan

This study was performed to find the composition area of cubic spinel-type monophase oxides composed of the Mn–Co–Ni ternary system. Starting materials were prepared by mixing Mn, Co, and Ni nitrates then evaporating to dryness. Each starting oxide was fired at 700, 800, 900, 1000, and 1100 °C in air. The regions of cubic spinel monophase (CSM) were confirmed to spread with decreasing firing temperatures. The region of CSM at 1000 °C was seen near the line connecting the points of Mn : Co : Ni = 2 : 4 : 0 and 4.5 : 0 : 1.5. The area at 800 °C spread toward Co and Ni, as compared to the results at 1000 °C. In the region containing more Mn above the area of CSM at 800 °C, the phase had tetragonal spinel or α-Mn_2O_3 besides cubic spinel structure. Below this area, the phase contained rock-salt-type crystal besides cubic spinel structure. This tendency at 1000 °C was the same as that at 800 °C.

1. Introduction

Some oxides consisting of transitional metals such as Mn, Co, and Ni are widely utilized as negative temperature coefficient (NTC) thermistor materials. Considering the diversified use of thermistors, further development of thermistor materials having compositions with electrical properties suitable for various purposes has been strongly desired. The oxide with spinel-type structure is considered to play an important role in electrical properties. Therefore, a method of preparing monophase oxide with cubic spinel-type structure is required in order to study the composition dependence of electrical properties and the electrical conduction mechanism.

The authors have studied NTC thermistor materials with specific compositions consisting of Mn–Co–Ni ternary system, and reported that the oxides fired at 1400 °C to sinter were not monophase but composed of cubic spinel-type, tetragonal spinel-type, and rock-salt-type oxides [1, 2]. For this reason, we investigated the preparation method of sintered bodies with monophase cubic spinel. We found that monophase with cubic spinel structure could be formed by oxidizing the oxide, which is a low rank oxide as a precursor, at temperatures where the spinel structure is stable [3, 4]. We named this process the PMSR (preparation of monophase spinel-type oxide through rock-salt-type oxide) method [5]. Using this method, we prepared monophase cubic spinel-type oxide with the following two systems: $Mn_{(2-x)}Co_{2x}Ni_{(1-x)}O_4$ ($0 \leqq X \leqq 1$) [5], and $Mn_{(2-2x)}Co_{3x}Ni_{(1-x)}O_4$ ($0 \leqq X \leqq 1$). It is important to examine the electrical properties of cubic spinel-type oxides over the wide composition region of the ternary system so that we can select elements to suit the purposes. However, the composition region where monophase is formed has been obscure except for the partial region described above. Accordingly, we must first determine the region of monophase with spinel structure in the ternary system.

This study was performed to comprehensively examine the stable phases of the ternary system at temperatures from 700 to 1100 °C, specifically to find the composition range of cubic spinel-type monophase.

2. Experimental

Starting materials for the compositions were prepared by mixing Mn, Co, and Ni nitrates then evaporating to dryness. About 0.6 g of each starting oxide was weighted into a platinum crucible and fired at 700, 800, 900, 1000, and 1100 °C in a vertically installed electrical furnace. The oxide was heated up to the prescribed temperature for 1 h and kept for 1, 3, and 16 h. In experiments at 700 °C, additional firing for 48 and 240 h was conducted. The experimental points examined are shown in Fig. 1. The firing atmosphere was air, and the fired specimen was dropped into water for quenching. The phases present in the specimens were analyzed by X-ray diffraction (XRD), and the crystal fractions in the specimens were calculated from the integrated peak intensities. In this calculation, the peaks of (311) for cubic spinel, (222) for α-Mn_2O_3 (Bixbyite), (200) for rock-salt-type oxide, (311) for tetragonal spinel, and (112) for γ-Mn_2O_3 were used. The peak areas of (311) and (113) for tetragonal spinel and those of (211) and (112) for γ-Mn_2O_3 were summed up, taking the multiplicity factor into account [6].

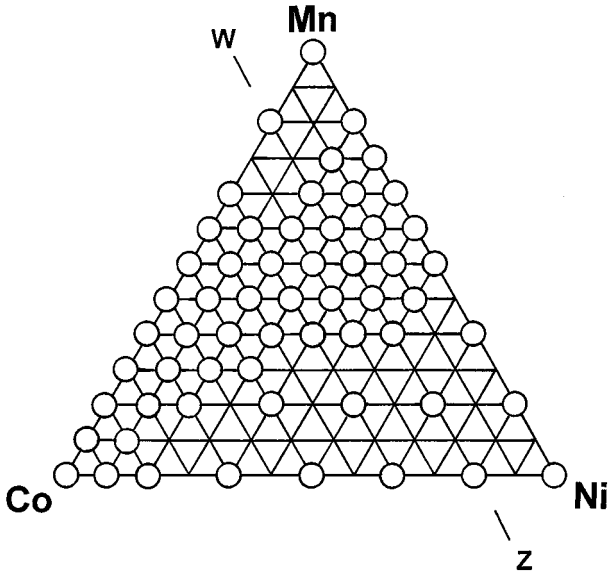

Figure 1 Composition diagram of Mn—Co—Ni.

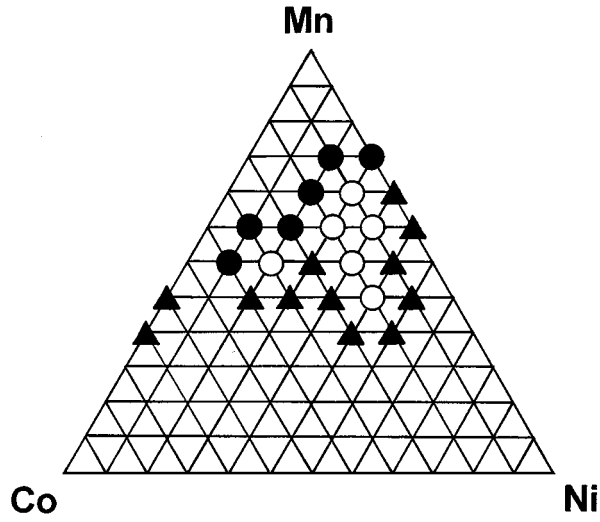

Figure 2 Phase relation in Mn—Co—Ni oxides fired at 1100 °C for 3 h. ○: cubic spinel, ●: cubic spinel and tetragonal spinel, ▲: cubic spinel and rock salt.

3. Results and discussion

The phases present in the specimens fired for 1, 3, and 16 h at 1000 °C were compared, to see the outline of the stable phase and to clarify the formation region of cubic spinel monophase (CSM). The formation region of CSM in the system 1 h-firing specimens was smaller than that in the 3 h-firing specimens. The region of CSM in the system 3 h-firing specimens was found to be the same as that in the system 16 h-firing specimens. In this paper, the phase diagrams at temperatures ranging from 800 to 1100 °C were thus revealed using the 3 h-firing data. In addition, we emphasized the phase diagram at 800 and 1000 °C in this study. The phases present at other temperatures (700, 900, and 1100 °C) were analyzed with limited components, focusing on the area of CSM formation.

3.1. Phases present in the oxides fired at 1100 °C

Fig. 2 shows the phase diagram at 1100 °C. XRD profiles are abbreviated here because the details are interpreted in the next section. As a result, the specimens with CSM were found to exist in the six components: Mn : Co : Ni = 3 : 2 : 1 3, 5 : 1 : 1.5, 3 : 1 : 2, 2.5 : 1 : 2.5, 4 : 0.5 : 1.5, and 3.5 : 0.5 : 2. This area of CSM seen at 1100 °C was the smallest in this experiment.

3.2. Phases present in the oxides fired at 1000 °C

Fig. 3 shows the result of the phase diagram obtained at 1000 °C. Fig. 4 illustrates the XRD patterns of the oxides of the binary system of Mn–Co. Profiles (a)–(g) correspond to the specimens with molar ratios of Mn : Co = 0 : 6, 1 : 5, 2 : 4, 3 : 3, 4 : 2, 5 : 1, and 6 : 0, respectively. The phase in the specimen consisting of only Co has a rock-salt-type structure (*R* phase), which is consistent with fact that CoO is known to be stable above 910 °C [7–10]. The phase in the specimen containing Mn of 17 mol % yields cubic spinel phase (*C* phase) besides *R* phase. The formation of CSM is recognized for the composition of Mn : Co = 2 : 4. The specimen of Mn : Co = 2.5 : 3.5 was also recognized to be composed of CSM. The XRD profile of the specimen was omitted because the profile was the same as that of the specimens with Mn : Co = 2 : 4. In the specimens containing Mn, one half or more, tetragonal spinel phase (*T* phase) becomes dominant. The oxide with the ratio of Mn : Co = 5 : 1 has γ-Mn_2O_3 type structure (*G* phase) instead of *C* phase. In the Mn oxide without Co, *G* phase is converted to α-Mn_2O_3 (*B* phase). The phases present in the region Mn : Co = 3 : 3 to Mn : Co = 6 : 0 are very similar to those reported by de Vidales *et al.* [11].

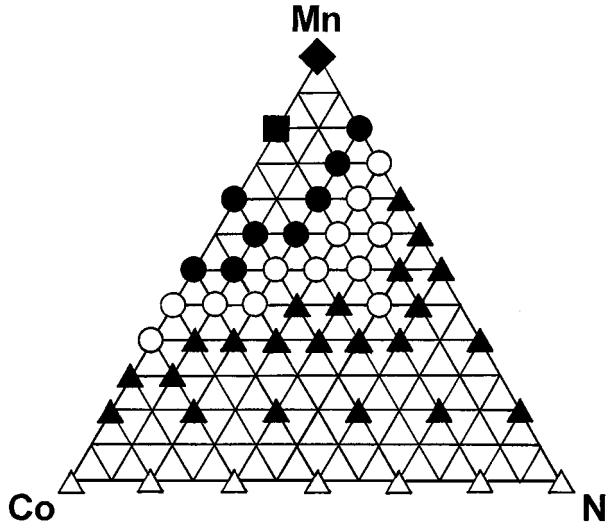

Figure 3 Phase relation in Mn—Co—Ni oxides fired at 1000 °C for 3 h. ○: cubic spinel, ●: cubic spinel and tetragonal spinel, ■: tetragonal spinel and γ-Mn_2O_3, ♦: tetragonal spinel and α-Mn_2O_3, ▲: cubic spinel and rock salt, △: rock salt.

In this paper hereafter the phase diagrams will be discussed based on the phases present in specimens, without showing XRD profiles. The oxides in the Co–Ni binary system were confirmed to be composed of only *R* phase. As is well known, CoO freely forms a solid solution with Ni oxide whose stable phase is NiO type [9, 10].

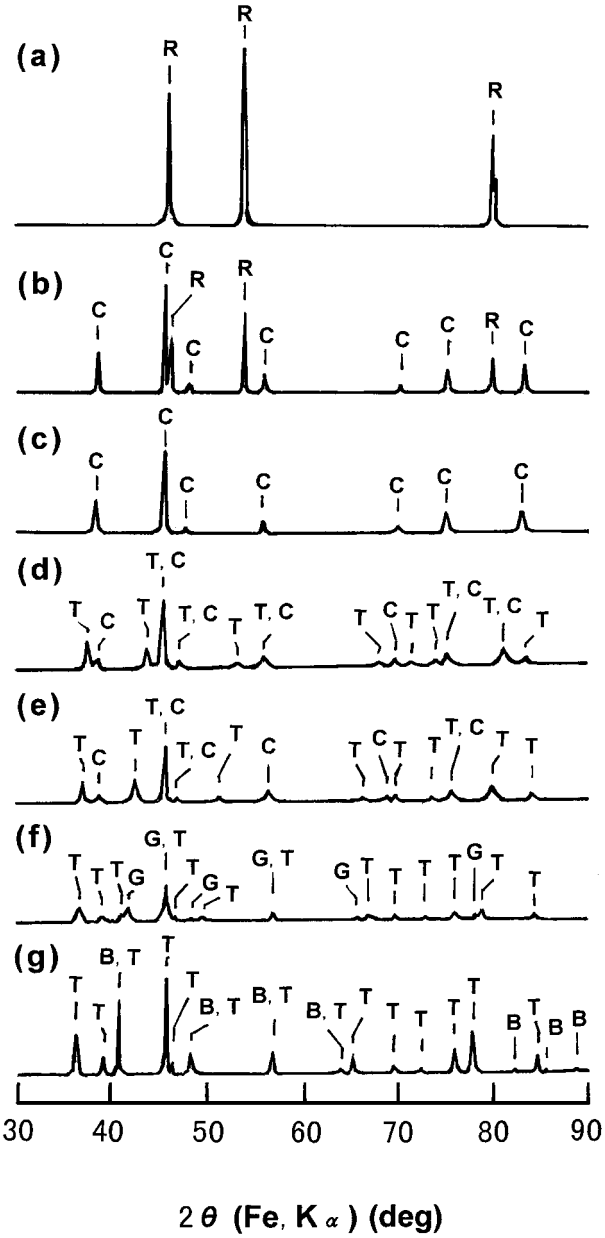

Figure 4 X-ray diffraction profiles of Mn—Co oxides fired at 1000 °C for 3 h. (a) Mn : Co = 0 : 6, (b) Mn : Co = 1 : 5, (c) Mn : Co = 2 : 4, (d) Mn : Co = 3 : 3, (e) Mn : Co = 4 : 2, (f) Mn : Co = 5 : 1, (g) Mn : Co = 6 : 0, *C*: cubic spinel, *R*: rock salt, *T*: tetragonal spinel, *G*: γ-Mn_2O_3, *B*: α-Mn_2O_3.

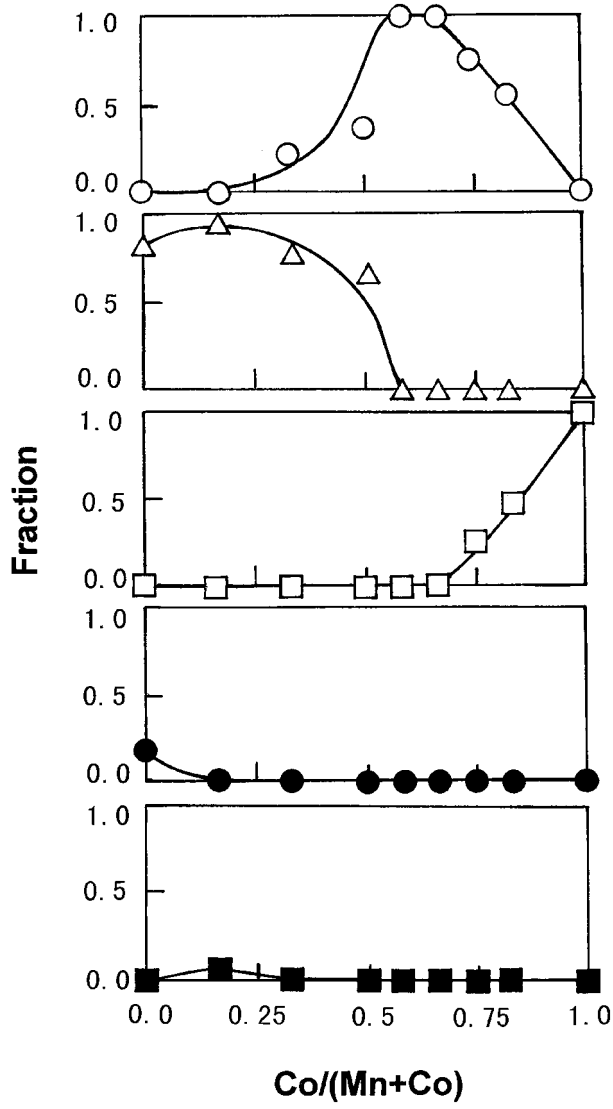

Figure 5 Fraction of each crystal phase in Mn—Co oxides fired at 1000 °C as a function of Co/(Mn + Co). ○: cubic spinel, △: tetragonal spinel, □: rock salt, ●: α-Mn_2O_3, ■: γ-Mn_2O_3.

The phases present in the oxides with compositions of the binary system Mn-Ni are composed of two crystal phases, except the oxides with Mn : Ni = 0 : 6 and 4.5 : 1.5. The specimens with Mn contain cubic and/or tetragonal spinel structure. CSM can be seen only at the composition of Mn : Ni = 4.5 : 1.5. In this binary system, the crystal structure with tetragonality is changed to cubic spinel structure as the Mn content decreases, which implies that the amount of Mn^{3+} occupying the octahedral site also decreases. In this case, Mn^{3+} causing Jahn-Teller distortion [12, 13] is considered to be replaced by Ni^{2+} which preferentially occupies the octahedral sites [14]. The area of CSM is seen on the line connecting the points of Mn : Co : Ni = 2 : 4 : 0 and 4.5 : 0 : 1.5. In the region above this line containing more Mn, the phase has tetragonal spinel besides cubic spinel structure. In contrast, below this line the phase contains rock-salt-type crystal besides cubic spinel structure. To see the changes of crystals in detail, the fractions of crystals in the specimens were evaluated from integrated peak intensities.

Fig. 5 shows the result obtained in the binary system of Mn—Co. The specimens with component of X = Co/(Mn + Co) ($0 \leqq X \leqq 0.17$) do not have crystals with cubic spinel structure. The phases present change from α-Mn_2O_3 and tetragonal spinel structure to γ-Mn_2O_3 and tetragonal spinel structure. The cubic spinel crystal appears in the specimen containing $X = 0.33$. The specimens with X between 0.58 and 0.67 are composed of cubic spinel structure. In the phases present in the specimens with X above 0.75, cubic spinel gradually decreases and rock-salt-type crystal appears. The specimen with $X = 1$ is revealed as CoO stable at 1000 °C. This series of crystal changes indicates that the valence of cations decreases in the direction of the Co end member.

In the ternary system containing CSM crystal, the specimens on the line W—Z shown in Fig. 1 were selected to check the changes in the crystal phase and

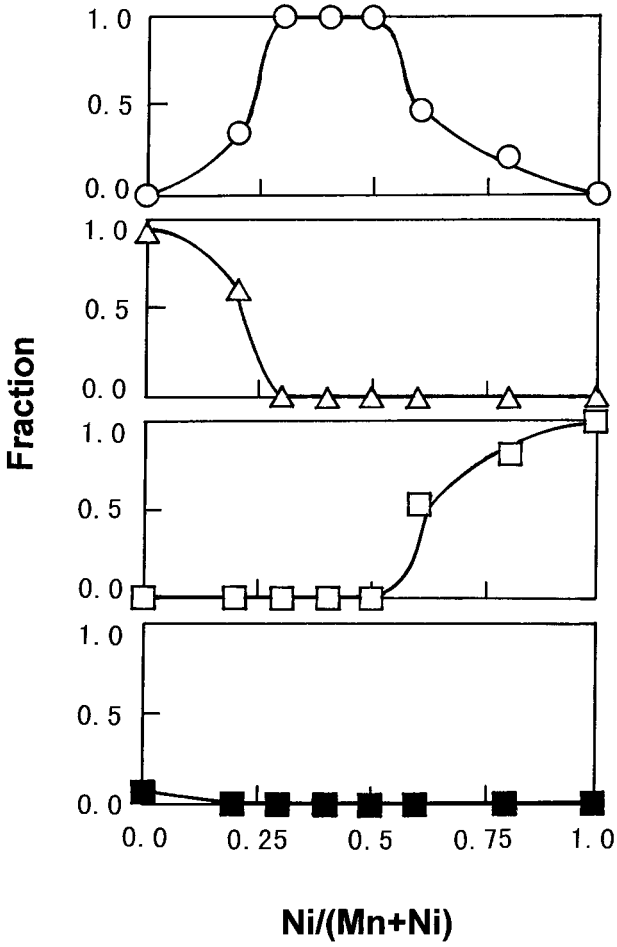

Figure 6 Fraction of each crystal phase in Mn—Co—Ni oxides fired at 1000 °C as a function of Ni/(Mn + Ni). ○: cubic spinel, △: tetragonal spinel, □: rock salt, ■: γ-Mn_2O_3.

fractions of each crystal. The fractions of each crystal in the specimens are shown in Fig. 6. In this case, the component of the specimens was treated using the figure of $Y = \mathrm{Ni}/(\mathrm{Mn} + \mathrm{Ni})$ because the content of Co was fixed. The specimen with $Y = 0$ has tetragonal spinel and γ-Mn_2O_3. The γ-Mn_2O_3 type crystal quantitatively is minor, and it disappears as Ni is contained. Cubic spinel-type crystal abruptly increases with increasing Ni content instead of decrease in tetragonal spinel-type crystal. For Y between 0.3 and 0.5, cubic spinel structure becomes dominant. The amount of cubic spinel crystal decreases above $Y = 0.6$, yielding rock-salt-type crystal. The phase present in the specimen with $Y = 1$ is composed of rock-salt-type structure. The oxides of the end members, Ni and Co, have rock-salt-type structures, whereas Mn oxides have spinel structures. The spinel structure exists until about $Y = 1$, which means that the structure is quite strong. Basically, the structure is considered to be stable as long as Mn^{3+} can be present in the octahedral site. Although it is natural for the tetragonality to disappear as Mn content decreases, the quantitative relation is obscure here because the cation distributions cannot be assigned yet. The concentration of Mn^{3+} which occupies 55% or less of the octahedral sites might be a criterion for judging the distortion disappearance [15, 16].

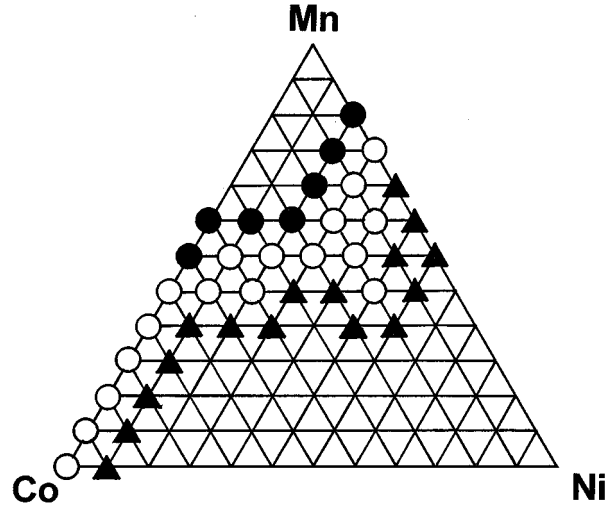

Figure 7 Phase relation in Mn—Co—Ni oxides fired at 900 °C for 3 h. ○: cubic spinel, ●: cubic spinel and tetragonal spinel, ▲: cubic spinel and rock salt.

3.3. Phases present in the oxides fired at 900 °C

Fig. 7 shows the phase diagram obtained at 900 °C. The region of CSM is somewhat wider than that at 1000 °C. Essentially, there is no large difference from the result of 1000 °C, except on the line of the Mn–Co binary system. It is characteristic that the region CSM spreads toward the Co on the line Mn–Co because the Co oxide does not have a rock-salt-type structure but a cubic spinel structure at 900 °C. It is known that CoO transforms into Co_3O_4 below 910 °C [7–10].

3.4. Phases present in the oxides fired at 800 °C

Fig. 8 shows the phase diagram obtained at 800 °C. It is clear that the region of CSM spreads toward Co and Ni compared with the results at 1000 and 900 °C. This suggests that the crystal of Co oxide determines

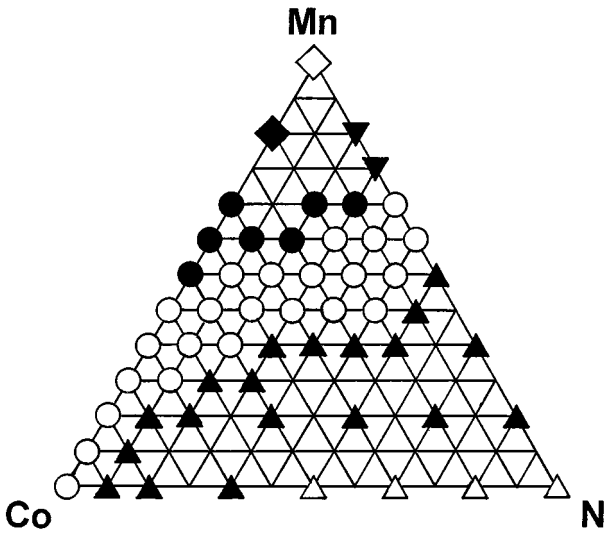

Figure 8 Phase relation in Mn—Co—Ni oxides fired at 800 °C for 3 h. ○: cubic spinel, ●: cubic spinel and tetragonal spinel, ▼: cubic spinel and α-Mn_2O_3, ♦: tetragonal spinel and α-Mn_2O_3, ◇: α-Mn_2O_3, ▲: cubic spinel and rock salt, △: rock salt.

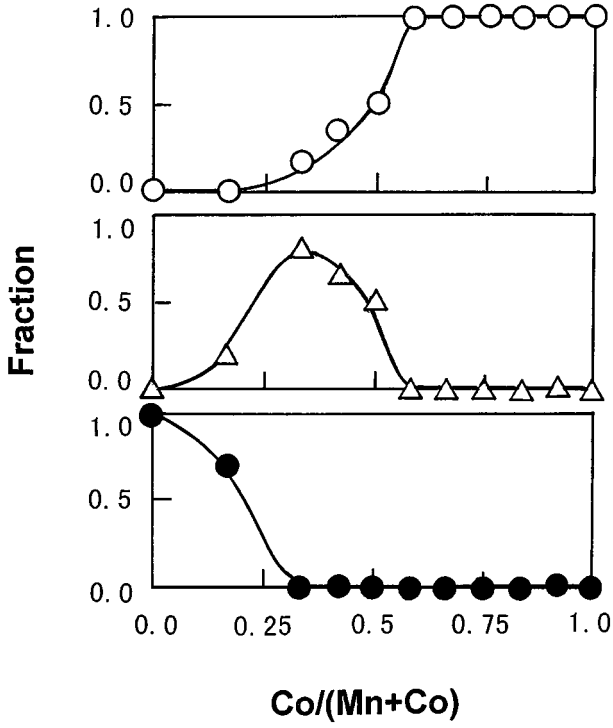

Figure 9 Fraction of each crystal phase in Mn—Co oxides fired at 800 °C as a function of Co/(Mn + Co). ○: cubic spinel, △: tetragonal spinel, ●: α-Mn_2O_3.

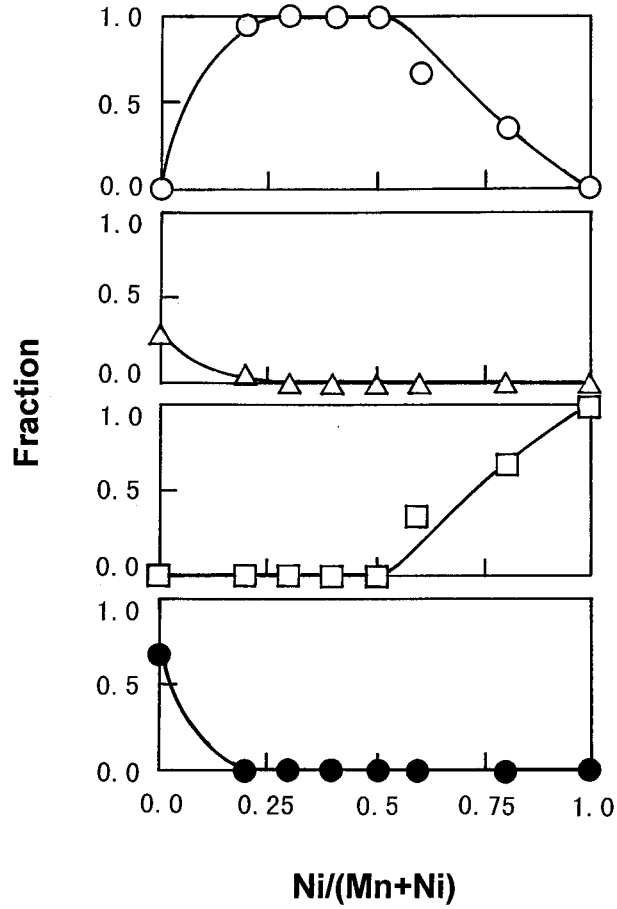

Figure 10 Fraction of each crystal phase in Mn—Co—Ni oxides fired at 800 °C as a function of Ni/(Mn + Ni). ○: cubic spinel, △: tetragonal spinel, □: rock salt, ●: α-Mn_2O_3.

the structure. Judging from the fact that the CSM is limited like a strip on the Mn–Co line, it seems difficult to react Co_3O_4 with NiO to obtain a solid solution. The difficulty of the solid solution formation excludes the possibilities that Ni^{2+} occupies the tetrahedral-site, and that Co^{3+} transfers to the tetrahedral-site due to octahedral-site replacement of Ni^{2+} which tends to prefer the octahedral-site. In the Mn-rich region above the CSM region, the crystal phase is complex corresponding to the content of Mn oxides. To see the crystal changes in detail, the fractions of crystals in the specimens were evaluated from integrated peak intensities in the same manner as that at 1000 °C.

Fig. 9 shows the relationship between fraction and X(=Co/(Mn + Co)) in Mn–Co binary specimens. For specimens in the range $0 \leqq X \leqq 0.17$, cubic spinel structure is absent. The phases present in the specimen with $X = 0.17$ are composed of α-Mn_2O_3 and tetragonal spinel structure. The cubic spinel crystal appears in the specimen with $X = 0.33$. The specimens with $X \geqq 0.58$ are composed of only cubic spinel structure. The CSM region is much wider than that in Fig. 5. This spreading is thought to be due to the Co oxide having cubic spinel structure at 800 °C.

Fig. 10 shows the relationship between the ratio of each crystal phase and Y(=Ni/(Mn + Ni)) in the same manner as that at 1000 °C. The existence ratio of α-Mn_2O_3 is large in the specimen with $Y = 0$. This result is fairly different from the result where the phase in the specimen with $Y = 0$ at 1000 °C is almost composed of tetragonal spinel. This seems to be because the phase present in the products is comprehensively determined by each crystal structure of Mn and Co oxides at 800 and 1000 °C. The oxide Mn_3O_4, which is mainly contained in the 1000 °C-specimen, can react with rock-salt-type CoO to form a solid solution because of the replacement of Mn^{2+} by Co^{2+}. However, the crystal phase of Mn oxide at 800 °C is α-Mn_2O_3. It is thought that the α-Mn_2O_3 reacts with spinel-type Co oxide to form a solid solution with a spinel structure. The specimen with $Y = 0.2$ is composed of a great amount of cubic spinel. In the region of Y between 0.3 and 0.5, cubic spinel structure becomes dominant. The amount of cubic spinel crystal decreases above $Y = 0.6$, yielding rock-salt-type crystal. The phase present in the specimen with $Y = 1$ is composed of a rock-salt-type structure. It is thought that the change in crystal phase is closely connected with the valence number of Mn and the stable phase of Ni oxide being NiO.

3.5. Phases present in the oxides fired at 700 °C

Fig. 11 shows the phase diagram of the specimens fired at 700 °C for 48 h. Two specimens with Mn : Co : Ni = 3 : 3 : 0 and 1 : 3 : 2 were fired for 240 h to examine whether the crystal phases differ from those of the 48 h-firing specimens, but the firing time appeared to have no effect. The phase diagram at 700 °C shown in Fig. 11 is inaccurate because minor specimens were selected for firing. However, the area of cubic spinel structure is considered to be almost the same as that at 800 °C.

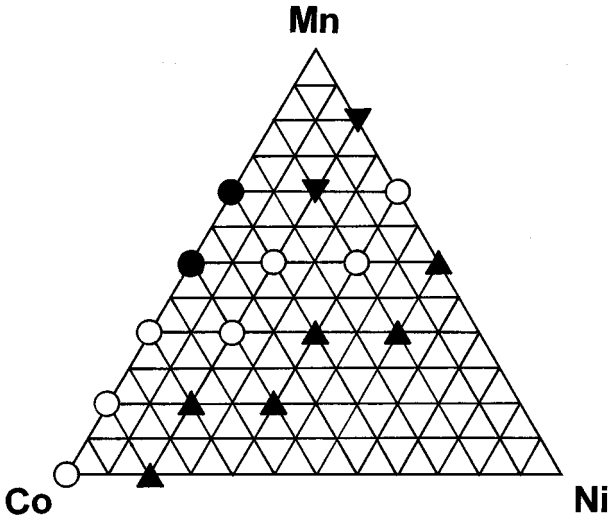

Figure 11 Phase relation in Mn—Co—Ni oxides fired at 700 °C for 48 h. ○: cubic spinel, ●: cubic spinel and tetragonal spinel, ▼: cubic spinel and α-Mn_2O_3, ▲: cubic spinel and rock salt.

4. Conclusions

This study was performed to investigate the composition area of cubic spinel-type monophase oxides composed of the Mn–Co–Ni ternary system, which is a prerequisite for preparing of sintering bodies consisting of monophase with cubic spinel structure by the PMSR method. The experiments were carried out at temperatures below sintering temperatures. The results are summarized as follows.

1. The region of cubic spinel monophase spreads with decreasing firing temperatures from 1100 to 800 °C.

2. The area of cubic spinel monophase at 1000 °C is seen near the line connecting the points of Mn : Co : Ni = 2 : 4 : 0 and 4.5 : 0 : 1.5. The area at 800 °C spreads toward Co and Ni as compared to the results at 1000 °C.

3. In the region containing more Mn above the area of cubic spinel monophase at 800 °C, the phase has tetragonal spinel or α-Mn_2O_3 besides cubic spinel structure. Below this area, the phase contains rock-salt-type crystal in addition to cubic spinel structure. This tendency at 1000 °C is the same as that at 800 °C.

References

1. T. MEGURO, T. SASAMOTO, T. YOKOYAMA, K. SHIRAISHI, Y. ABE and N. TORIKAI, *J. Ceram. Soc. Jpn.* **96** (1988) 334.
2. T. YOKOYAMA, T. MEGURO, T. SASAMOTO, S. YAMADA, Y. ABE and N. TORIKAI, *ibid.* **96** (1988) 967.
3. T. MEGURO, T. YOKOYAMA and K. KOMEYA, *J. Mater. Sci.* **27** (1992) 5529.
4. T. YOKOYAMA, K. KONDO, K. KOMEYA, T. MEGURO, Y. ABE and T. SASAMOTO, *ibid.* **30** (1995) 1845.
5. T. YOKOYAMA, Y. ABE, T. MEGURO, K. KOMEYA, K. KONDO, S. KANEKO and T. SASAMOTO, *Jpn. J. Appl. Phys.* **35** (1996) 5775.
6. L. V. AZÁROFF and M. J. BUERGER, "The Powder Method in X-ray Crystallography" (McGraw-Hill, New York, 1958) p. 181.
7. E. AUKRUST and A. MUAN, *Trans. Metallurgical Soc. AIME* **230** (1964) 378.
8. E. M. LEVIN, C. R. ROBBINS and H. F. MCMURDIE, "Phase Diagrams for Ceramists," Vol. II (edited and published by Amer. Ceram. Soc., OH, 1969) p. 22.
9. R. J. MOORE and J. WHITE, *J. Mater. Sci.* **9** (1974) 1393.
10. R. S. POTH, T. NEGAS and L. P. COOK, "Phase Diagrams for Ceramists," Vol. IV, edited by G. Smith (Amer. Ceram. Soc., OH, 1981) p. 30.
11. J. L. M. DE VIDALES, E. VILA, R. M. ROJAS and O. GARCIA MARTINEZ, *Chem. Mater.* **7** (1995) 1716.
12. J. D. DUNITZ and L. E. ORGEL, *J. Phys. Chem. Solids* **3** (1957) 20.
13. P. J. WOJTOWICZ, *Phys. Rev.* **116** (1959) 32.
14. T. YOKOYAMA, T. MEGURO and K. KOMEYA, *J. Mater. Sci. Soc. Jpn.* **33** (1996) 19.
15. L. V. AZÁROFF, *Z. Kristallogr.* **B112** (1959) 33.
16. N. BAFFIER and M. HUBER, *J. Phys. Chem. Solids* **33** (1972) 737.

Received 13 November 1998
and accepted 15 March 1999